Cosmologically Probing Ultra-light Particle Dark Matter using 21 cm Signals

Yi Mao[1], *Kenji Kadota*[2,3], *Kiyomoto Ichiki*[4] *and Joseph Silk*[1,5,6]

[1] Institut d'Astrophysique de Paris, Institut Lagrange de Paris, CNRS, UPMC Univ Paris 06, UMR7095, 98 bis, boulevard Arago, F-75014, Paris, France
[2] Department of Physics, Nagoya University, Nagoya 464-8602, Japan
[3] Center for Theoretical Physics of the Universe, Institute for Basic Science, Daejeon 305-811, Korea
[4] Kobayashi-Maskawa Institute for the Origin of Particles and the Universe, Nagoya University, Nagoya 464-8602, Japan
[5] The Johns Hopkins University, Department of Physics and Astronomy, Baltimore, Maryland 21218, USA
[6] Beecroft Institute of Particle Astrophysics and Cosmology, University of Oxford, Oxford OX1 3RH, UK

DOI: http://dx.doi.org/10.3204/DESY-PROC-2014-03/mao_yi

Ubiquitous ultra-light scalar fields may make a partial contribution to the dark matter and affect the large scale structure of the Universe. While their properties are heavily model dependent, we develop a model-independent analysis to forecast the constraints on their mass and abundance using futuristic 21 cm observation as well as CMB lensing measurements. We demonstrate that the 21 cm power spectrum are most sensitive to the ultra-light dark matter with mass $m \sim 10^{-26}$ eV for which the precision attainable on mass and abundance bounds can be of the order of a few percent.

1 Introduction

The existence of light scalar fields has been explored from both particle phenomenology and cosmological aspects. As an astrophysical example, the ultra-light particles (ULPs) with mass of the order of the current Hubble scale $H_0 \approx 2 \times 10^{-33}$ eV [1] may contribute to a small fraction of the total matter in our Universe. Those ultra-light scalar fields can have an imprint on the matter power spectrum due to *free-streaming*, similar to that due to massive neutrinos. Since the range of possible mass is wide, so is the range of the suppression scale in the matter power spectrum. In this proceeding paper, we forecast cosmological constraints on two free parameters of the ULPs, their mass and abundance, with CMB lensing and futuristic 21 cm observations. We aim to clarify the range of the mass and abundance of ULPs which 21 cm observations will be most sensitive to.

In what follows, §2 outlines the effect of the ULPs on the matter power spectrum. §3 gives a brief review of the Fisher forecast formalism, followed by the results in §4. The main results

[1] Throughout this paper, the mass is in units of $H_0 \approx 2 \times 10^{-33}$ eV.

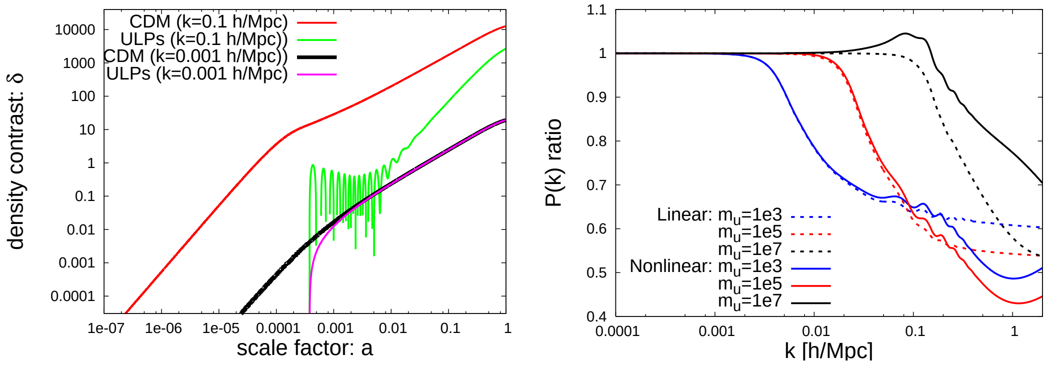

Figure 1: (Left) The evolution of perturbations for ULPs ($m_u = 10^5 H_0, f_u = 0.05$) and for CDM only. (Right) The ratio of the power spectrum $P(k)$ with ULPs ($f_u = 0.05$) to that with CDM only. Figures are reused from [1].

of this proceeding have been published in [1].

2 Suppression in the Matter Power Spectrum

For the leading order perturbation equation, $\ddot{\delta}_k + 2H\dot{\delta}_k + \left(\frac{c_s^2 k^2}{a^2} - 4\pi G\rho_m\right)\delta_k = 0$, there exists a gravitationally stable solution for short wave-length mode $k \gg k_J$ and an unstable (growing) one for $k \ll k_J$, with the Jeans wave number $k_J = (a/c_s)\sqrt{4\pi G\rho_m}$. For the ULPs, its effective sound speed is $c_s \approx k/2m_u a$ for $a \gg k/2m_u$, and $c_s \approx 1$ below the Compton scale $a \ll k/2m_u$, where m_u is the ULP mass [2, 3]. Therefore, $k_J(a) = 2a(\pi G\rho_m(a))^{1/4} m_u^{1/2}$ for $a \gg k/2m_u$. We consider scenarios in this paper where the ULP behaves like dark energy due to the large Hubble friction for $H > m_u$, and starts oscillations like dark matter, once $H \leq m_u$. We implement ULPs into CAMB [4] accordingly. The evolution of the ULP fluctuations $\delta_u = \delta\rho_u/\rho_u$ is shown in the left panel of Fig. 1 for the ULP mass and fraction $m_u = 10^5 H_0$, $f_u = \Omega_u/\Omega_m = 0.05$. The fluctuations $\delta(k)$ cannot grow when they behave like a cosmological constant and can start growing once the ULPs start to oscillate. The perturbation growth however is suppressed inside the Jeans scale and the perturbation growth has to wait till it goes outside the Jeans scale for a large enough value of a. We also plotted the CDM perturbation evolution which illustrates that the ULP perturbations can catch up with the CDM perturbations for small k but not for large k, analogously to the well-known behavior of the baryon perturbation evolution. The nonlinearity becomes important when $k^3 P(k)/(2\pi^2)$ becomes of order unity. We estimate that $m_u \sim 10^5 H_0$ leads to the oscillation starting around the matter-radiation equality epoch $z_{osc} \sim 3200(\sim z_{eq})$. For the modes which enter the horizon during matter domination, the suppression in the matter power spectrum starts around the scale corresponding to the Jeans scale when the ULP starts oscillating $k \sim \left(H_0^2\Omega_m\right)^{1/3} m_u^{1/3}$. Similarly, when the oscillations start during radiation domination, the suppression is expected to occur for scales smaller than the Jeans scale at matter-radiation equality $k \sim (m_u^2 H_0^2 \Omega_m a_{eq})^{1/4}$. The suppression scales for different masses are illustrated in the right panel of Fig. 1 which shows the transfer function

$T^2(k) = P(k)_{\rm ULPs}/P(k)_{\rm no\ ULPs}$ representing the ratio of the power spectrum including the ULPs to that without ULPs. We are particularly interested in the ULP masses which affect the matter power at the 21 cm-observable scales of $0.055 \lesssim k \lesssim 0.15$ Mpc^{-1}. We can see that the baryon acoustic oscillation effects are more prominent in the nonlinear matter power spectrum than in the linear one and $m_u \sim 10^7 H_0$ lets the suppression start right in the 21 cm observable range.

3 Forecast Formalism

To forecast the constraints on the cosmological parameters including those relevant to the ULPs, we perform the Fisher likelihood analysis for future 21 cm experiments. We also use the CMB observables including CMB lensing which help remove the parameter degeneracies that the 21 cm signals would otherwise suffer from. We briefly outline the formalism of the likelihood analysis here, and present the results in the next section.

The 21 cm radiation comes from the atomic transition between the two hyperfine levels of the hydrogen $1s$ ground state. In the linear regime, the power spectrum of 21 cm brightness temperature fluctuations can be written as $P_{\Delta T}(\mathbf{k}, z) = \widetilde{\delta T_b}^2 \, \overline{x}^2_{H_I}[b_{H_I}(z) + \mu^2_{\mathbf{k}}]^2 \; P_{\delta\delta}(k, z)$, where $\widetilde{\delta T_b}(z) = (23.88\text{mK}) \left(\frac{\Omega_b h^2}{0.02}\right) \sqrt{\frac{0.15}{\Omega_m h^2}\frac{1+z}{10}}$. Here we consider $z \lesssim 10$ when the spin temperature $T_S \gg T_{CMB}$. We define the neutral and ionized density bias, $b_{H_I}(z)$ and $b_{H_{II}}(z)$, as $b_{H_I} \equiv \delta_{\rho_{H_I}}(k)/\delta_\rho(k)$, $b_{H_{II}} \equiv \delta_{\rho_{H_{II}}}(k)/\delta_\rho(k)$. They are related by $b_{H_I} = (1 - \overline{x}_{H_{II}} b_{H_{II}})/\overline{x}_{H_I}$. We use the excursion set model of reionization [5] to obtain the fiducial values of ionized density bias $b_{H_{II}}(z)$ and the mean ionized fraction $\overline{x}_{H_{II}}(z)$. The Fisher matrix for 21 cm power spectrum measurements is [6, 7] $F^{21\rm cm}_{\alpha\beta} = \sum_{\mathbf{u}} \frac{1}{[\delta P_{\Delta T}(\mathbf{u})]^2} \left(\frac{\partial P_{\Delta T}(\mathbf{u})}{\partial p_\alpha}\right) \left(\frac{\partial P_{\Delta T}(\mathbf{u})}{\partial p_\beta}\right)$, where $\{p_\alpha\}$ represents the free parameters in our model. We assume a logarithmic pixelization $du_\perp/u_\perp = du_\parallel/u_\parallel = 0.1$. The error in power spectrum measurement is $\delta P_{\Delta T}(\mathbf{u}) = [P_{\Delta T}(\mathbf{u}) + P_N(u_\perp)]/\sqrt{N_c}$, where $N_c = u_\perp du_\perp du_\parallel \Omega B/(2\pi^2)$ is the number of independent modes in each pixel (Ω is a field of view solid angle and B is the bandwidth of a redshift bin). P_N is the noise power spectrum $P_N(\mathbf{u}_\perp, z) = (\lambda T_{sys}/A_e)^2/(t_0 n(\mathbf{u}_\perp))$, where $T_{sys} \approx (280\text{K})[(1 + z)/7.4]^{2.3}$ is the system temperature [8], A_e is the effective collecting area of each antenna tile, and t_0 is the total observation time. We assume an Omniscope-like instrument [9] consisting of a million 1m $\times$ 1m dipole antennae with a field of view of 2π steradians and we assume $t_0 = 4000$ hours for each redshift bin of bandwidth $B = 6$MHz. We also assume the residual foregrounds can be neglected for $k_\parallel \geq k_{\parallel,\min} = 2\pi/(yB)$ [6], and the minimum baseline L_{min} sets $k_{\perp,\min} = 2\pi L_{min}/(\lambda d_A)$ (for example, for an Omniscope-like array, $k_{min} \approx k_{\parallel,\min} = 0.055\,\text{Mpc}^{-1}$ at $z = 10.1$). We conservatively restrict our studies to large scale $k \leq 0.15\,\text{Mpc}^{-1}$ for the sake of the linear treatment of 21 cm observables, to avoid any scale-dependent bias at the nonlinear regime and the nonlinear effects due to reionization patchiness at the scale of the typical size of ionized regions [10].

The CMB can also be affected by light dark matter through the change in matter-radiation equality and also via the Sachs-Wolfe effect. The CMB is also helpful in removing the degeneracies among the cosmological parameters. The CMB lensing is in particular helpful in removing the so-called geometric degeneracy which the primary CMB observables would otherwise suffer from. We consider the CMB observables T, E, d which represent the CMB temperature, polarization and CMB deflection angle respectively. We assume the Planck-like specifications [11]

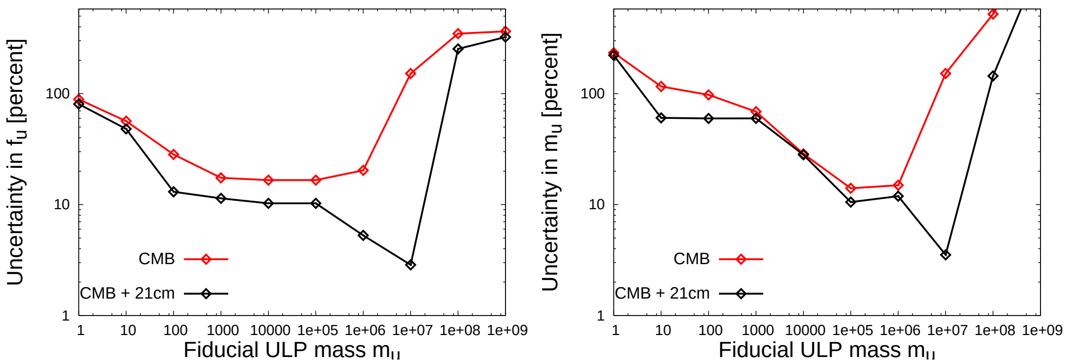

Figure 2: 1σ errors in f_u (left) and m_u (right) for several fiducial values of m_u in units of $H_0 \approx 2 \times 10^{-33}$ eV, with fiducial value $f_u = 0.05$. Figures are reused from [1].

including the CMB lensing measurements covering up to the multipole $l_{max} = 2500$, three channels $100, 143, 217$ GHz and the sky coverage $f_{sky} = 0.65$. The Fisher matrix for CMB lensing is $F^{CMB}_{\alpha\beta} = \sum_{l=2}^{l_{max}} \frac{f_{sky}(2l+1)}{2} Tr[\mathbf{C}_{,\alpha}\, \mathbf{C}^{-1} \mathbf{C}_{,\beta}\, \mathbf{C}^{-1}]$, where $_{,\alpha}$ refers to the partial derivative with respect to a cosmological parameter p_α, and $\mathbf{C}$ is the covariance matrix. We assume the noise in the auto-correlation spectra is dominated by detector noise represented by the photon shot noise [12, 13], and the CMB lensing statistical noise is estimated using the optimal quadratic estimator method of Hu & Okamoto [14, 15]. The total Fisher matrix was obtained by adding the 21 cm and CMB Fisher matrix $F \approx F^{21cm} + F^{CMB}$. The modified version of the CAMB [4] was used to obtain the CMB and matter power spectra where the ultra-light fluid component was implemented in the Boltzmann equations.

4 Results

We vary 12 parameters in our Fisher analysis Ω_Λ, $\Omega_m h^2$, $\Omega_b h^2$, n_s, A_s (scalar amplitude), τ (reionization optical depth), N_{eff} (the effective number of relativistic neutrino species), m_u (mass of ULPs), f_u (ratio of ULP abundance to total matter), f_ν (ratio of neutrino abundance to total matter), $x_{H_I}(z)$ (mean neutral fraction at redshift z), $b_{H_{II}}(z)$ (H II density bias at redshift z). For the fiducial models, unless stated otherwise, we use $x_{H_I} = 0.5$ at the redshift bin of $z = 10.10$ and $b_{H_{II}} = 5.43$ obtained by the excursion set model of reionization [5], and the power spectrum up to the scale $k_{max} = 0.15\,\mathrm{Mpc}^{-1}$ was used.

Our main results are summarized in Fig. 2 which shows the 1σ uncertainties in the ULP parameters for several representative ULP masses for $f_u = 0.05$. The 1σ errors on the ULP parameters f_u, m_u can be of order a few percent for the mass range, around $m_u \sim 10^7 H_0$, to which the 21 cm signals are most sensitive. This ULP mass lets the ULPs start oscillations at $0.055 \lesssim k \lesssim 0.15\mathrm{Mpc}^{-1}$ which, as Fig. 1 shows, is where the matter power spectrum has the significant change with respect to that of the CDM only. On the other hand, the sensitivity of the CMB observables to the ULPs increases up to the ULP mass of about $10^5 H_0$ which corresponds to the oscillation starting around the CMB last scattering epoch. For instance, we found numerically $2 \times 10^4 H_0 \sim H(z = 1100)$ and we can indeed see that $\sigma(m_u)$ does not improve so much by adding the 21 cm observables for the mass around $m_u \sim 10^{4\sim5}H_0$. This implies that the CMB constraint on m_u is dominant over that from the 21 cm observables for this mass range. The CMB, however, starts losing its sensitivity to the ULPs significantly for the larger ULP masses $m_u \gtrsim 10^6 H_0$ which initiate the oscillations well before the last scattering epoch.

In short, we find that the CMB measurements are most sensitive to the ULP mass range of $10^4 H_0 \sim 10^6 H_0$, and the 21 cm measurements are most sensitive to $m_u \sim 10^7 H_0$. We forecast that the future 21 cm can constrain the ULP density fraction and the mass with an accuracy of the order of a few percent. Because of the complications due to nonlinearity, however, the ULPs with $m_u \gg 10^7 H_0$ would be hard to probe by the large-scale structure of the Universe, even though these mass ranges can be well probed by other probes such as black holes and dwarf galaxies. Further studies on the complementarity between different observables are left for future work.

Acknowledgments

We thank K. Choi and D. Marsh for the useful discussions. This work was supported by the MEXT of Japan and by French state funds managed by the ANR within the Investissements d'Avenir programme under reference ANR-11-IDEX-0004-02. The research of JS has been supported at IAP by the ERC project 267117 (DARK) hosted by Université Pierre et Marie Curie - Paris 6 and at JHU by NSF grant OIA-1124403. K.K. thanks the hospitality of IAP where this work was initiated.

References

[1] K. Kadota, Y. Mao, K. Ichiki and J. Silk, JCAP **1406**, 011 (2014) [arXiv:1312.1898 [hep-ph]].

[2] W. Hu, R. Barkana and A. Gruzinov, Phys. Rev. Lett. **85**, 1158 (2000) [astro-ph/0003365].

[3] W. Hu, Astrophys. J. **506**, 485 (1998) [astro-ph/9801234].

[4] A. Lewis, A. Challinor, A. Lasenby Astrophys. J. **538**, 473 (2000) [astro-ph/9911177].

[5] S. Furlanetto, M. Zaldarriaga and L. Hernquist, Astrophys. J. **613**, 1 (2004) [astro-ph/0403697].

[6] M. McQuinn, O. Zahn, M. Zaldarriaga, L. Hernquist and S. R. Furlanetto, Astrophys. J. **653**, 815 (2006) [astro-ph/0512263].

[7] Y. Mao, M. Tegmark, M. McQuinn, M. Zaldarriaga and O. Zahn, Phys. Rev. D **78**, 023529 (2008) [arXiv:0802.1710 [astro-ph]].

[8] S. Wyithe and M. F. Morales, [astro-ph/0703070 [ASTRO-PH]].

[9] M. Tegmark and M. Zaldarriaga, Phys. Rev. D **82**, 103501 (2010) [arXiv:0909.0001 [astro-ph.CO]], M. Tegmark and M. Zaldarriaga, Phys. Rev. D **79**, 083530 (2009) [arXiv:0805.4414 [astro-ph]].

[10] P. R. Shapiro, Y. Mao, I. T. Iliev, G. Mellema, K. K. Datta, K. Ahn and J. Koda, Phys. Rev. Lett. **110**, 151301 (2013) [arXiv:1211.2036 [astro-ph.CO]].

[11] P. A. R. Ade *et al.* [Planck Collaboration], arXiv:1303.5062 [astro-ph.CO].

[12] J. R. Bond, G. Efstathiou and M. Tegmark, Mon. Not. Roy. Astron. Soc. **291**, L33 (1997) [astro-ph/9702100].

[13] L. Knox, Phys. Rev. D **52**, 4307 (1995) [astro-ph/9504054].

[14] W. Hu and T. Okamoto, Astrophys. J. **574**, 566 (2002) [astro-ph/0111606].

[15] T. Okamoto and W. Hu, Phys. Rev. D **67**, 083002 (2003) [astro-ph/0301031].